Clinical Cancer Research

Molecular Subtypes of Pulmonary Large-cell Neuroendocrine Carcinoma Predict Chemotherapy Treatment Outcome

Jules L. Derks[1], Noémie Leblay[2], Erik Thunnissen[3], Robert Jan van Suylen[4], Michael den Bakker[5], Harry J.M. Groen[6], Egbert F. Smit[7], Ronald Damhuis[8], Esther C. van den Broek[9], Amélie Charbrier[2], Matthieu Foll[2], James D. McKay[2], PALGA-Group, Lynnette Fernandez-Cuesta[2], Ernst-Jan M. Speel[10], and Anne-Marie C. Dingemans[1]

Abstract

Purpose: Previous genomic studies have identified two mutually exclusive molecular subtypes of large-cell neuroendocrine carcinoma (LCNEC): the *RB1* mutated (mostly comutated with *TP53*) and the *RB1* wild-type groups. We assessed whether these subtypes have a predictive value on chemotherapy outcome.

Experimental Design: Clinical data and tumor specimens were retrospectively obtained from the Netherlands Cancer Registry and Pathology Registry. Panel-consensus pathology revision confirmed the diagnosis of LCNEC in 148 of 232 cases. Next-generation sequencing (NGS) for *TP53, RB1, STK11,* and *KEAP1* genes, as well as IHC for RB1 and P16 was performed on 79 and 109 cases, respectively, and correlated with overall survival (OS) and progression-free survival (PFS), stratifying for non–small cell lung cancer type chemotherapy including platinum + gemcitabine or taxanes (NSCLC-GEM/TAX) and platinum-etoposide (SCLC-PE).

Results: *RB1* mutation and protein loss were detected in 47% ($n = 37$) and 72% ($n = 78$) of the cases, respectively. Patients with *RB1* wild-type LCNEC treated with NSCLC-GEM/TAX had a significantly longer OS [9.6; 95% confidence interval (CI), 7.7–11.6 months] than those treated with SCLC-PE [5.8 (5.5–6.1); $P = 0.026$]. Similar results were obtained for patients expressing RB1 in their tumors ($P = 0.001$). RB1 staining or P16 loss showed similar results. The same outcome for chemotherapy treatment was observed in LCNEC tumors harboring an *RB1* mutation or lost RB1 protein.

Conclusions: Patients with LCNEC tumors that carry a wild-type *RB1* gene or express the RB1 protein do better with NSCLC-GEM/TAX treatment than with SCLC-PE chemotherapy. However, no difference was observed for *RB1* mutated or with lost protein expression. *Clin Cancer Res; 24(1); 33–42. ©2017 AACR.*

Introduction

Large-cell neuroendocrine carcinoma (LCNEC) is a high-grade neuroendocrine carcinoma with non–small cell cytologic features that accounts for 1% to 3% of all lung cancers (1, 2). Similar to small-cell lung cancer (SCLC), LCNEC is a disease with a poor prognosis (2, 3). The diagnosis of LCNEC requires assessing both morphology and neuroendocrine differentiation by IHC (4, 5). Previously, we and others have shown that separation of LCNEC from SCLC and pulmonary carcinoids can be difficult even on resection specimens (6–10). In the current WHO classification, some of the features used to classify a tumor as LCNEC overlap with those applied for SCLC, NSCLC, and carcinoids (8).

To improve the separation of LCNEC from carcinoids on a biopsy specimen, the proliferation marker Ki-67 with a cutoff >20% was proposed (10); however, the differential diagnosis between LCNEC and SCLC remains an issue for pathologists, due to crush artefacts, distorted cytologic features of SCLC on large

[1]Department of Pulmonary Diseases, GROW School for Oncology & Developmental Biology, Maastricht University Medical Centre, Maastricht, the Netherlands. [2]Genetic Cancer Susceptibility Group, International Agency for Research on Cancer (IARC-WHO), Lyon, France. [3]Department of Pathology, VU University Medical Centre, Amsterdam, the Netherlands. [4]Pathology-DNA, Jeroen Bosch Hospital, s' Hertogenbosch, the Netherlands. [5]Department of Pathology, Maasstad hospital, Rotterdam, the Netherlands. [6]Department of Pulmonary Diseases, University of Groningen and University Medical Centre, Groningen, the Netherlands. [7]Department of Pulmonary Diseases, VU medical centre, Amsterdam, the Netherlands. [8]Department Research, Comprehensive Cancer Association, Utrecht, the Netherlands. [9]PALGA Foundation, Houten, the Netherlands. [10]Department of Pathology, GROW school for Oncology & Developmental Biology, Maastricht University Medical Centre, Maastricht, the Netherlands.

Note: Supplementary data for this article are available at Clinical Cancer Research Online (http://clincancerres.aacrjournals.org/).

L. Fernandez-Cuesta, E.-J. Speel, and A.-M.C. Dingemans contributed equally to this article.

Current address for M. den Bakker: Maasstad Hospital, Rotterdam, the Netherlands; and current address for Egbert F. Smit: Department of Thoracic Oncology, Netherlands Cancer Institute, Amsterdam, the Netherlands.

Corresponding Authors: Anne-Marie C. Dingemans, Department of Pulmonology, P. Debyelaan 25, Post-box 5800 6202 AZ, Maastricht. Phone: 314-3387-1318; Fax: 314-3387-5051; E-mail: a.dingemans@mumc.nl; and Lynnette Fernandez-Cuesta, International Agency for Research on Cancer, 150, cours Albert Thomas, Lyon 69008, France. E-mail: fernandezcuestal@iarc.fr

doi: 10.1158/1078-0432.CCR-17-1921

Translational Relevance

Large-cell neuroendocrine carcinoma (LCNEC) is a rare subtype of lung cancer for which the optimal treatment in advanced disease is debated (i.e., non-small cell lung cancer (NSCLC) versus small-cell lung cancer (SCLC) type chemotherapy regimen). In this study, which is the largest stage IV LCNEC patients cohort ($n = 79$) with information about chemotherapy treatment outcome, analyzed by next-generation sequencing, we tested in the two recently identified molecular subtypes of LCNEC (*RB1* and *TP53* mutated or *STK11/KEAP1* and *TP53* mutated) are valuable for treatment decision. Our results indicate that patients with LCNEC tumors that harbor a wild-type and/or express RB1 have superior overall survival when treated with NSCLC chemotherapy compared with SCLC chemotherapy. These data strengthen the relevance for molecular profiling in LCNEC, besides the oncogenic alterations already screened for in routine practice (e.g., EGFR).

tissue samples (11), tumor heterogeneity (11), and overlap in cell and nuclear size between LCNEC and SCLC (9). This is further worsened by the fact that, at diagnosis, both SCLC and LCNEC are often metastasized, and commonly only one biopsy specimen is available for diagnosis (12). The identification of diagnostic markers to allow separation of LCNEC from SCLC is therefore an unmet need.

Chemotherapy treatment for LCNEC is a subject of debate since it seems to be less chemosensitive than SCLC. In the American Society of Clinical Oncology (ASCO) guideline, either platinum–etoposide chemotherapy (SCLC-PE) treatment or the same regimen as for non–small cell nonsquamous cell carcinoma is advised for LCNEC (13), although SCLC-PE is considered as the most appropriate (13). Nevertheless, recent studies indicate that patients with LCNEC have a more favorable outcome when treated with platinum–gemcitabine or taxane chemotherapy (NSCLC-GEM/TAX) compared with SCLC-PE (14–16). The molecular characteristics that may explain these differences in the response to different chemotherapies remain unknown.

Several next-generation sequencing (NGS) studies have shown that LCNEC tumors can be further subdivided into two mutually exclusive groups based on their mutational patterns (17, 18): one harboring inactivation of *TP53* and *STK11* and/or *KEAP1* genes, and the other one enriched for inactivation of *TP53* and *RB1*, a hallmark of SCLC. It has been hypothesized that these LCNEC subtypes may require different chemotherapy treatment (17). In this study, we tested whether the described molecular LCNEC subtypes may have an impact on the chemotherapy response.

Materials and Methods

Regulations

The study protocol was approved by the medical ethical committee of the Maastricht University Medical Centre (METC azM/UM 14-4-043) and performed according to the Dutch "Federa, Human Tissue and Medical Research: Code of conduct for responsible use (2011)" regulations not requiring patient informed consent.

Patient and tumor selection

In this retrospective population-based study, all data were retrieved from the Netherlands Cancer Registry and Netherlands Pathology Registry (PALGA, the nationwide registry of pathology in the Netherlands; ref. 19) as previously described (12). Data managers from the cancer registry retrospectively updated (2015) clinical data of all first-line chemotherapy-treated stage IV LCNEC patients ($n = 232$, Fig. 1). Available data included clinical characteristics, TNM stage, overall survival (OS), and progression-free survival (PFS) from date of diagnosis until first evidence of progression, death or last day of follow-up, and chemotherapy details. All patients received platinum doublet (cisplatin or carboplatin) chemotherapy treatment, further divided into three groups: "NSCLC-GEM/TAX" including gemcitabine, docetaxel, or paclitaxel; "NSCLC-PEM" including pemetrexed; and "SCLC-PE" including etoposide. NSCLC-PEM chemotherapy was separated from the other NSCLC regimens because of previously reported resistance in (large cell) neuroendocrine carcinomas (14, 20–23).

Panel consensus pathology revision

From all histologic specimens, the original hematoxylin and eosin (HE) and IHC slides were collected. Subsequently, three pathologists (R.J. van Suylen, E. Thunnissen, M. den Bakker), who were blinded for clinical outcome, systematically scored all cases at a multi-head microscope for WHO 2015 criteria. Proliferative activity was evaluated by estimation of MIB1 and mitotic counting (mitoses/2 mm^2; ref. 8). The MIB1 (Ki-67) staining was scored (<25%, >25%) when available (10, 24). Either >10 mitosis/2 mm^2, abundant tumor necrosis, or a Ki-67 staining of >25% of tumor cells was sufficient to score for high-grade tumor (19, 24). Diagnoses were considered as consensus when at least two pathologists agreed, further referred to as panel consensus. All panel consensus LCNEC tumors were included for NGS and IHC staining analysis when formalin-fixed paraffin embedded (FFPE) tissue block(s) were available ($n = 109$; Fig. 1).

DNA isolation

Tumor macrodissection was performed aiming at a tumor cell content of at least 20%. DNA was extracted from four to eight 10-μm slides using the Maxwell FFPE LEV Automated DNA Extraction Kit (Promega Corporation). DNA concentration was measured using the QuantiFluor dsDNA Dye System (Promega Corporation).

Amplicon design and target enrichment

One hundred and sixty-nine amplicons of 150 base pairs (bp) in size were designed using the Qiagen GeneRead DNAseq Custom V2 Builder tool reference CNGHS-02445X-169 (GRCh37) covering the following exons: *TP53*, *RB1*, *STK11*, and *KEAP1*. This custom GeneRead amplicon-based custom panel covered 100% of the coding region (i.e., exonic) of *TP53*, 95% of *RB1*, 81% of *STK11*, and 95% of *KEAP1*. A validated in-house protocol (IARC) was used to perform multiplex PCR with four separate primer pools. Per pool, 5 μL of DNA diluted to a maximum of 4 ng/μL (0.60–4.0) were dispensed and air-dried. Subsequently, 5 μL of the PCR mix were added (containing 2.5 μL primer, 1 μL PCR mix, 0.34 μL HotStar Taq, and 1.16 μL H_20) and the DNA was amplified in a 384-well plate as following: 15 minutes at 95°C, and 25 cycles of 15 seconds at 95°C and 4 minutes at 60°C, and 10 minutes at 72°C. After amplification, the PCR products were pooled into a single reaction per sample.

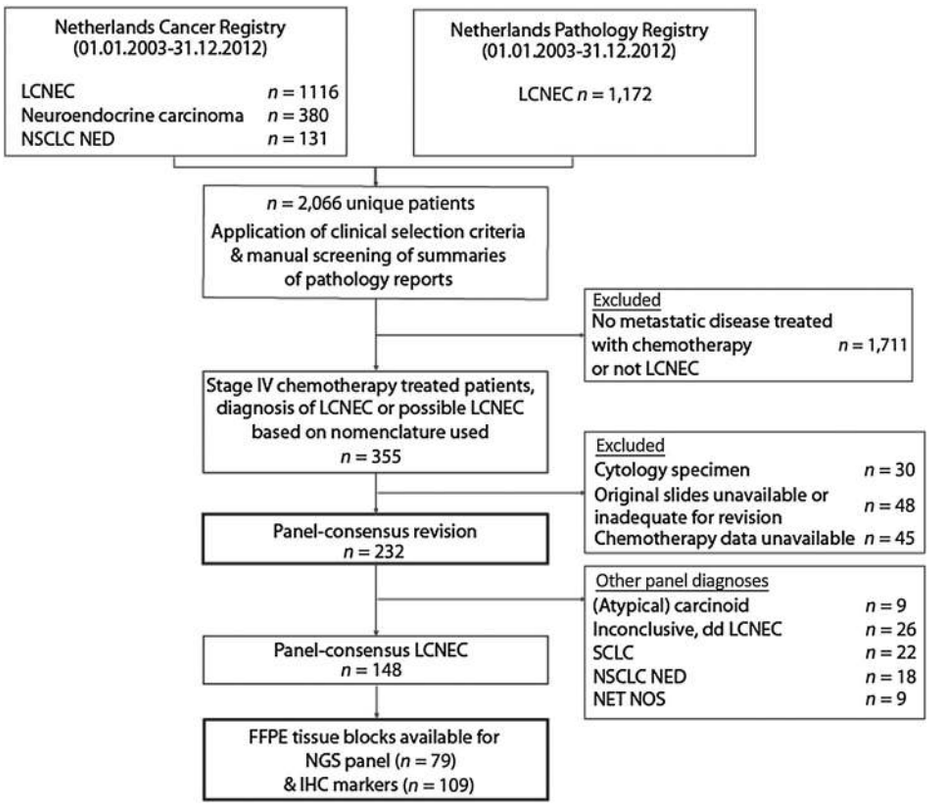

Figure 1.
Selection of patients and tumor slides for panel-consensus review and molecular analyses. Abbreviations: N, number; NSCLC NED, non-small cell lung carcinoma with IHC neuroendocrine differentiation; NET NOS, neuroendocrine tumor not otherwise specified.

Library preparation and next-generation sequencing

The amplified PCR products were purified using NucleoMag NGS Clean-up and Size Select beads (Macherey-Nagel). Purified PCR products were quantified by Qubit DNA high-sensitivity assay kit (Invitrogen Corporation). A minimum of 100 ng of purified PCR product was included for library preparation with the NEBNext Fast DNA Library Prep Set (New England BioLabs, USA) following an in-house validated protocol (IARC). End-repair was performed and ligated to specific adapters and in-house prepared individual barcodes (Eurofins MWG Operon). Bead purification was applied to clean libraries and amplification was performed. Equimolarly pooled libraries were loaded on a 2% agarose gel for electrophoresis (220 V, 40 minutes). Using the GeneClean Turbo kit (MP Biomedicals) DNA fragments of 110 to 220 bp were recovered from the pooled libraries. Library quality and quantity were assessed on the Agilent 2100 Bioanalyzer on-chip electrophoresis (Agilent Technologies). Sequencing was performed on the Ion Torrent Proton Sequencer (Life Technologies Corp.), aiming for a minimum coverage of 250×, using the Ion PI Hi-Q OT2 200 Kit and the Ion PI Hi-Q sequencing 200 Kit with the Ion PI chip V3 (Life Technologies Corp.), following manufacturer's instructions.

Technical duplicates and bioinformatical analysis

Technical duplicates were included for all samples and processed in identical 96- and 384-well plates to prevent PCR errors. Sequencing data were aligned to the hg19 (GRCh37) reference genome and BAM files were generated using the Torrent Suite Software (v4.4.2). For all amplicon positions, the read depth was calculated using SAMtools (25) and samples with a median coverage lower than 250× were excluded. Needlestack (https://github.com/IARCbioinfo/needlestack; ref. 26) was used to call variants with default parameters except for the base-quality and the mapping-quality thresholds (10 and 1, respectively). Annotation was performed with ANNOVAR (27) using the PopFreqAll (popfreq_all_20150413), COSMIC v77, SIFT and Polyphen (dbnsfp30a) databases (28, 29). We only considered those mutations identified by Needlestack in the two technical duplicates. In addition, we excluded the ones with an allelic fraction lower than 5%, a relative-variant strand bias (RVSB) higher than 0.85, or those already reported as germline in any of the ExAC, ESP or 1000G populations with a frequency larger than 0.001 (30–32). In addition, all mutations had to either be (i) reported in the COSMIC database, or (ii) damaging mutations (ii) damaging mutations (stop, indels and splice), or (iii), missense mutations classified as deleterious by SIFT or Polyphen databases (Supplementary Data File S1; NGS data).

RB1 and P16 IHC and scoring

The N-terminal and C-terminal regions of the RB1 protein were targeted with antibody 4H1 (1:100, Cell Signaling Technology) and 13A10 (1:100, Leica Biosystems). In addition, the protein P16 was targeted with antibody JC8 (1:400, Santa Cruz Biotechnology). Three-micron-thick FFPE slides were stained using a Dako Autostainer Link 48 system with the EnVision FLEX visualization Kit (DAKO, Agilent) according to the standard protocols. For 13A10 and JC8 high-pH antigen retrieval was used, and for 4H1 low-pH antigen retrieval was used. Tonsillar tissue (control for P16/RB1) and tumor stromal cells (internal control for RB1) were included as positive controls. H-scores were calculated as a total score of the percentage of tumor cells with staining intensity 1 (weak nuclear staining) ×1, intensity 2 (moderate

nuclear staining) ×2, and intensity 3 (strong nuclear staining) ×3 with a maximum score of 300. H-scores were evaluated for all RB1 and P16 markers by E-J. M. Speel who was blinded for all clinical, histopathologic, and mutational data.

FISH

To detect homozygous deletions of the *RB1* gene, FISH was performed with the ZytoLight SPEC RB1/13a12 Dual Color Probe (Zytovision). Three-micron-thick sections were cut from FFPE tumors without a detectable *RB1* mutation but with loss of RB1 protein expression. FISH slides were deparaffinized, air dried at room temperature, pretreated with 0.2 mol/L HCL for 20 minutes at room temperature, followed by incubation in 1 mol/L NaSCN for 30 minutes at 80°C. Subsequently, sections were treated with pepsin from porcine stomach mucosa (Sigma-Aldrich; 0.5 mg/mL in 0.14 mol/L NaCl pH 2), postfixed in 1% formaldehyde in PBS for 10 minutes, and dehydrated in 70% to 100% ethanol. The ZytoLight SPEC RB1/13a12 Dual Color Probe was added under a coverslip (undiluted, 6–10 μL). Denaturation of probe and target DNA was carried out simultaneously for 5 min at 85°C before hybridization overnight at 37°C in a humid chamber (Thermobrite). After removing the coverslips, slides were stringently washed to remove unhybridized probe in 2× SSC/0.3% NP40 at pH 7.0 at 73°C for 2 minutes. Slides were dehydrated in an ascending ethanol series (70%–100%) and mounted in 0.2 μg/mL DAPI-Vectashield (Vector Laboratories). Probe signals were scored using a DM 5000 B fluorescence microscope (Leica) with specific filter sets for rhodamine-, fluorescein-, and DAPI.

Each tumor was screened for the presence/absence of *RB1* (orange) and *13q12* (green) signals, and the predominant copy number per nucleus was noted (e.g., 1:1, 1:2, 2:2). Normal tonsillar tissue and internal normal tissue parts in the tumor tissue served as internal controls with a predominant 2:2 pattern. A homozygous deletion was considered when no *RB1* (orange) signal was observed in the tumor tissue. All cases were evaluated by J. Derks and E.-J. M. Speel.

Statistical analysis

All analyses were performed using SPSS (version 22 for Windows, Inc.). The χ^2 and Fisher exact test were used to compare categorical data; the Wilcoxon signed-rank test was used for continuous variables. OS and PFS were analyzed using two-sided log-rank test and survival curves were estimated using the Kaplan–Meier method. To evaluate the predictive role of *RB1* mutation and IHC status, a Cox regression model was used including an interaction term for the marker and the chemotherapy treatment. Two-sided *P* values <0.05 were considered significant.

Results

Pathology revision and molecular characterization by next-generation sequencing

A panel of three expert pathologists (R.J. van Suylen, E. Thunnissen, and M. den Bakker) reviewed the 232 clinically annotated and initially classified as stage IV LCNEC, available in the Netherlands Pathology Registry. In total, 148 of them were confirmed as panel consensus LCNEC tumors (Fig. 1; Supplementary Data File S1). The fact that tumors reclassified as carcinoids ($n = 9$) had a longer survival than those confirmed as LCNEC ($P = 0.008$) supports the value of the pathology revision (Supplementary Fig. S1A and S1B). Of the 148 confirmed LCNECs, 79 tumors passed the quality controls for NGS analyses and were targeted sequenced for the coding regions of *TP53*, *RB1*, *KEAP1*, and *STK11* (Supplementary Data File S1).

We obtained a median coverage of 2,850× (range, 261–6,870) per sample. Mutations in *TP53* were present in 85% of the cases ($n = 67$), *RB1* in 47% ($n = 37$), *KEAP1* in 18% ($n = 14$), and *STK11* in 10% ($n = 8$); five samples were wild-type for the four genes analyzed (Fig. 2). *RB1* was coaltered with

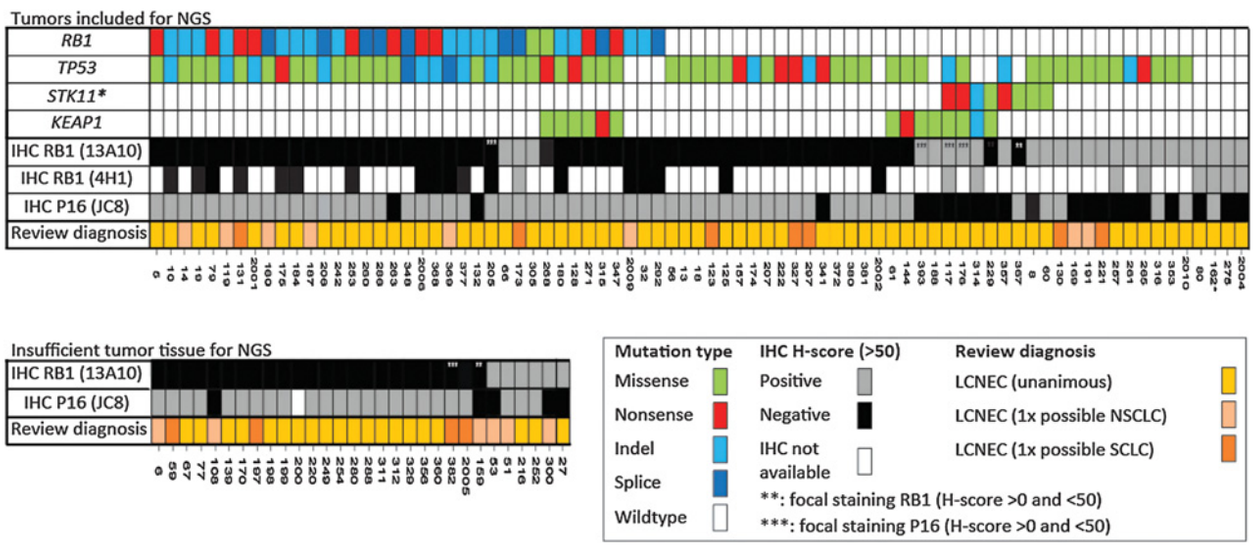

Figure 2.

Overview of genomic profiles of the LCNEC cases analyzed by targeted exon sequencing of the *RB1, TP53, STK11, KEAP1* genes and by IHC for RB1 and P16. In total, 79 LCNEC tumors were sequenced, and an additional set of 30 were only analyzed by IHC. *, In tumor sample 162 the DNA was isolated from tissue obtained 10 months after initiation of treatment.

Table 1. Clinical characteristics of patients included for NGS and IHC analyses

	NGS			*P*	IHC			*P*
Clinical characteristics	**Total**	**RB1^{wt}**	**RB1^{mt}**	**^{wt} vs. ^{mt}**	**Total**	**RB1^{+}**	**RB1^{-}**	**$^{+}$ vs. $^{-}$**
Total patients included, *n*	79	42	37		109	31	78	
Age (median, IQR)[a]	65 (51–79)	64 (46–82)	65 (53–77)	0.87	64 (59–79)	64 (52–76)	63 (48–78)	0.99
Gender				0.37				0.33
Male	51 (65)	29 (69)	22 (59)		66 (61)	21 (68)	45 (58)	
Female	28 (35)	13 (31)	15 (41)		43 (39)	10 (32)	33 (42)	
Chemotherapy clusters				0.91[b]				0.56[b]
NSCLC-GEM/TAX	31 (39)	15 (35)	16 (43)		45 (41)	14 (45)	31 (40)	
SCLC-CE	28 (35)	13 (31)	15 (41)		40 (37)	9 (29)	31 (40)	
NSCLC-PEM	13 (17)	7 (17)	6 (16)		15 (14)	3 (10)	12 (15)	
Unknown	7 (9)	7 (17)	0 (0)		9 (8)	5 (16)	4 (5)	
Chemotherapy subtypes				–				–
Gemcitabine	22 (28)	11 (26)	11 (30)		35 (32)	9 (29)	26 (35)	
Taxanes (docetaxel/paclitaxel)	9 (11)	4 (9)	5 (14)		10 (9)	5 (16)	5 (7)	
Etoposide	28 (35)	13 (30)	15 (40)		40 (37)	9 (29)	31 (41)	
Pemetrexed	13 (16)	7 (17)	6 (16)		15 (14)	3 (10)	12 (16)	
Unknown	7 (9)	7 (17)	0 (0)		9 (8)	5 (16)	1 (1)	
Cycles of chemotherapy				0.47[c]				0.56[c]
1	9 (11)	5 (12)	4 (11)		17 (16)	5 (16)	12 (15)	
2	13 (17)	5 (12)	8 (22)		13 (12)	2 (7)	11 (14)	
3	12 (15)	5 (12)	7 (19)		14 (13)	5 (16)	9 (12)	
4	34 (43)	20 (47)	14 (37)		49 (45)	13 (42)	36 (46)	
>4	9 (11)	5 (12)	4 (11)		13 (12)	4 (13)	9 (12)	
Unknown	2 (3)	2 (5)	0 (0)		3 (3)	2 (6)	1 (1)	
Second-line chemotherapy treatment				0.99				0.21
No	64 (81)	34 (81)	30 (81)		89 (82)	23 (74)	66 (85)	
Yes	15 (19)	8 (19)	7 (19)		20 (18)	8 (26)	12 (15)	

Abbreviations: IQR, interquartile range; wt, wild-type; mt, mutation.
[a]Wilcoxon signed-rank test.
[b]Excluded unknown cases for comparison.
[c]Excluded unknown cases for comparison, compared ≤2 vs. >2 cycles.

TP53 in 34 of the 37 *RB1*-mutated tumors; *RB1* mutations were mutually exclusive with *STK11* $P = 0.006$ but not with *KEAP1* mutations $P = 0.71$.

Clinical relevance of the mutational patterns of LCNEC tumors

The clinical characteristics of the patients, which tumors were sequenced, are shown in Table 1: median age was 64 (range, 51–79), 65% were males, 55% completed first-line chemotherapy (≥4 cycles), and 19% received second-line chemotherapy treatment. When considering only the patients with available data on the subtype of chemotherapy ($n = 72$, 91%), we observed that those LCNEC tumors that harbored a wild-type *RB1* gene showed a significant longer OS when treated with NSCLC-GEM/TAX compared with SCLC-PE [(9.6; 95% confidence interval (CI), 7.7–11.6 versus 5.8 (95% CI, 5.5–6.1) months, $P = 0.026$] and to NSCLC-PEM chemotherapy [6.7 (95% CI, 5.1–8.2), $P = 0.039$; Fig. 3A)]. No difference was observed in the case of LCNECs with an *RB1* mutation (Fig. 3B). Using a Cox regression model, the presence of a wild-type *RB1* was associated with a significant difference (HR, 2.37; 95% CI, 1.09–5.19) favoring NSCLC-GEM/TAX chemotherapy over SCLC-PE treatment. However, comparison of the overall group did not identify a significant interaction between the *RB1* mutational status and the chemotherapy treatment ($P = 0.35$; Fig. 4).

The PFS of *RB1* wild-type NSCLC-GEM/TAX–treated patients was also significantly higher compared with treatment with SCLC-PE [6.1 (95% CI, 4.2–8.0) months versus 5.7 (95% CI, 3.9–7.6), $P = 0.019$] but similar to treatment with NSCLC-PEM [4.7 (95% CI, 3.0–6.4), $P = 0.18$; Supplementary Fig. S2A]. Similarly to OS, no difference was observed for PFS in *RB1*-mutated LCNEC patients for the different chemotherapy regimens (Supplementary Fig. S2B). Finally, the mutational status of none the assessed genes (*TP53*, *RB1*, *STK11*, *KEAP1)* had a prognostic value (Fig. 5A–D).

Correlation between mutational patterns and IHC analyses

We assessed the RB1 protein expression levels by IHC in all of the 79 tumors sequenced (Fig. 2) and found that 92% of the *RB1*-mutated LCNEC tumors had an RB1 H-score of 0 [the median was 0 (range, 0–200) compared with the internal controls; Supplementary Fig. S3A]. The three cases that retained RB1 expression carried two splice mutations and one single nucleotide variation, all reported in COSMIC, respectively (Supplementary Data File S1). No difference was observed regarding the C- and N-terminal RB1 protein staining when stratifying by type of mutation (splice/indel/single nucleotide variants).

In LCNEC tumors with *RB1* wild-type, the median H-score was 50 (range, 0–200; Fig. 2; Supplementary Data File S1, Supplementary Fig. S3C). In 18 (43%), the H-score was 0. To test whether a copy-number alteration was the underlying mechanism for this loss of expression, we performed FISH in the 16 cases for which tissue was available (Supplementary Data File S1). However, no homozygous deletion was found in any of the samples suggesting alternate mechanisms for *RB1* inactivation, such as genomic rearrangements or large deletions detectable with the techniques used in this study.

Considering the reported interobserver variation in the diagnosis of SCLC and LCNEC, and the fact that virtually all SCLCs carry an inactivated *RB1* (33), we evaluated whether there was a correlation between the panel diagnosis and the loss of RB1 protein expression. In total, we performed IHC analyses on

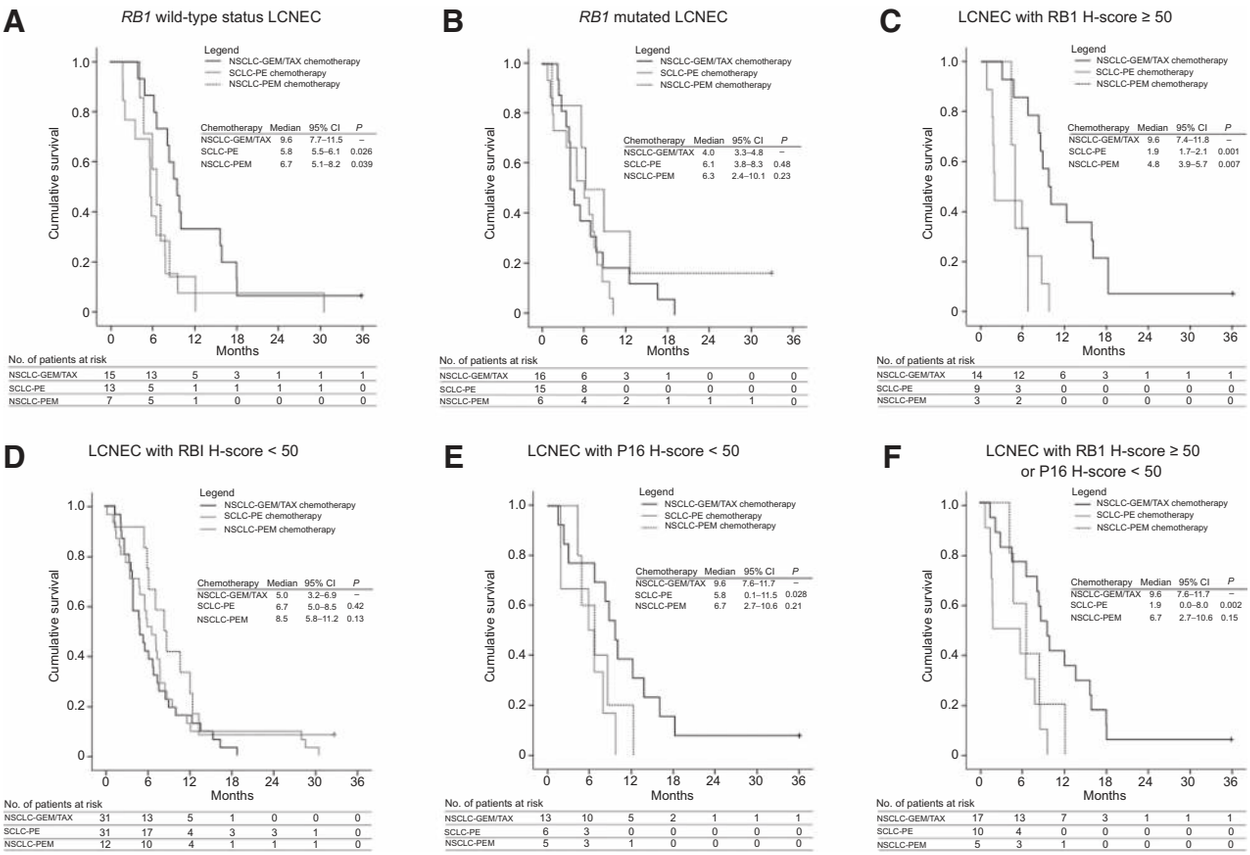

Figure 3.

Overall survival for subtypes of chemotherapy in panel consensus LCNEC with *RB1* wild-type* (**A**), *RB1* mutation (**B**), H-score ≥50 for RB1* IHC (**C**), H-score <50 for RB1 IHC (**D**), H-score <50 for P16 IHC (**E**), and H-score ≥50 for RB1* or <50 for P16 on IHC analysis (**F**). Abbreviations: No, number of. *, case 162 excluded from analyses.

109 panel consensus diagnosed LCNEC. For 98 of them, the panel unanimously diagnosed the tumors as LCNEC but for 11, one of the pathologists classified the tumor as SCLC. We did not observe a significant difference in the prevalence of RB1 expression in these 11 cases (27% with an H-score >50) when comparing with the 98 LCNEC unanimously classified (29% with an H-score >50, $P = 0.93$).

Previous studies have identified a correlation between *RB1* inactivation, loss of expression, and, P16 expression (34, 35). We, therefore, analyzed our series of samples for P16 protein expression and found that, while the median P16 H-score in the *RB1* wild-type LCNEC group was 180 (range, 0–300), this value went up to 300 (range, 0–300) in the *RB1*-mutated cases (Fig. 2; Supplementary Fig. S3B). In total, 91% of the LCNEC tumors with a P16 H-score <50 harbored a wild-type *RB1* gene (Fig. 2; Supplementary Fig. S3D).

Clinical relevance of the IHC results

Patients with LCNEC showing an RB1 H-score ≥50 had a significant longer OS when treated with NSCLC-GEM/TAX than with SCLC-PE [9.6 (95% CI, 7.4–11.8) vs. 1.9 (95% CI, 1.7–2.1) months, $P = 0.001$] or NSCLC-PEM [4.8 (95% CI, 3.9–5.7) months, $P = 0.007$; Fig. 3C]. Cox regression analysis confirmed the predictive value of RB1-positive staining on NSCLC-GEM/TAX versus SCLC-PE chemotherapy outcome (HR 4.96; 95% CI, 1.79–13.74, $P_{interaction} = 0.002$; Fig. 4). PFS was also significantly longer for NSCLC-GEM/TAX versus SCLC-PE–treated patients [5.5 (95% CI, 1.9–9.0) and 1.7 (95% CI, 0.0–4.8) months ($P = 0.023$), respectively] but not versus NSCLC-PEM [4.1 (95% CI, 4.0–4.2) months, $P = 0.21$; Supplementary Fig. S2C]. No statistically significant difference in response to different chemotherapy treatments was observed in patients with LCNEC tumors with an RB1 H-score <50, independently of their mutational status (Fig. 3D; Supplementary Fig. S2D).

P16 IHC H-score <50 was correlated with improved OS for NSCLC-GEM-TAX versus SCLC-PE chemotherapy ($P = 0.028$; Fig. 3D) but it had no impact on PFS ($P = 0.24$; Supplementary Fig. S2D). Combined evaluation of RB1 H-score ≥50 and/or P16 <50 showed identical results for OS ($P = 0.002$; Fig. 3F) and PFS ($P = 0.027$; Supplementary Fig. S2F). Similarly to the mutational status, none of the RB1 and P16 H-scores had prognostic value (Fig. 5E and F).

Discussion

Once diagnosed, LCNEC is frequently treated with SCLC-PE chemotherapy, with poor responses (13, 14, 36, 37). Recently, we

Cox-regression analysis and test for interaction for mutation status, type of chemotherapy treatment related to overall survival

Variable	NSCLC GEM/TAX (n)	SCLC PE (n)	Hazards ratio (95% CI)[a]	Interaction *P*-value[b]
RB1-mutated	16	15	1.31 (0.62–2.77)	0.35
RB1 wild-type	15	13	2.37 (1.09–5.19)	
RB1 (<50 H-score)	31	31	0.81 (0.48–1.36)	0.002
RB1 (>= 50 H-score)	14	9	4.96 (1.79–13.74)	

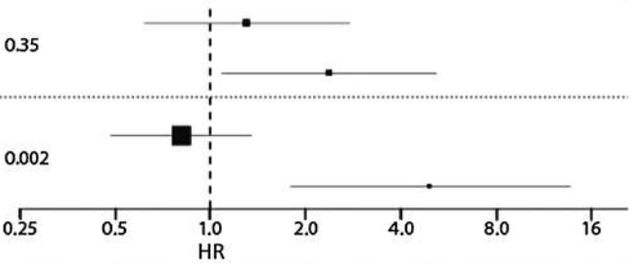

a: Cox-regression model for covariate treatment (NSCLC-GEM/TAX versus SCLC-PE) within group with variable specified (e.g. all *RB1*-mutated LCNEC)
b: Cox-regression model including the covariate treatment (NSCLC-GEM/TAX versus SCLC-PE) and variable specified including an intraction term for treatment*variable (e.g. *RB1* mutation type*treatment)

Figure 4.
Cox regression model for overall survival including the covariates *RB1* and chemotherapy. A test for interaction was performed to evaluate the predictive value of *RB1* mutations and RB1 protein expression measured by IHC, for chemotherapy outcome.

provided evidence that NSCLC-GEM/TAX chemotherapy may perform better than SCLC-PE chemotherapy on LCNEC tumors (14). Here we have tested whether the molecular characteristics of the LCNEC tumors might explain these differences.

In line with what has been already reported (17, 18, 38), *TP53* was found mutated in 85% of our LCNEC cases, *RB1* in 47%, *KEAP1* in 18%, and *STK11* in 10%. *RB1* was coaltered with *TP53* in 92% of the *RB1*-mutated tumors, and mutations

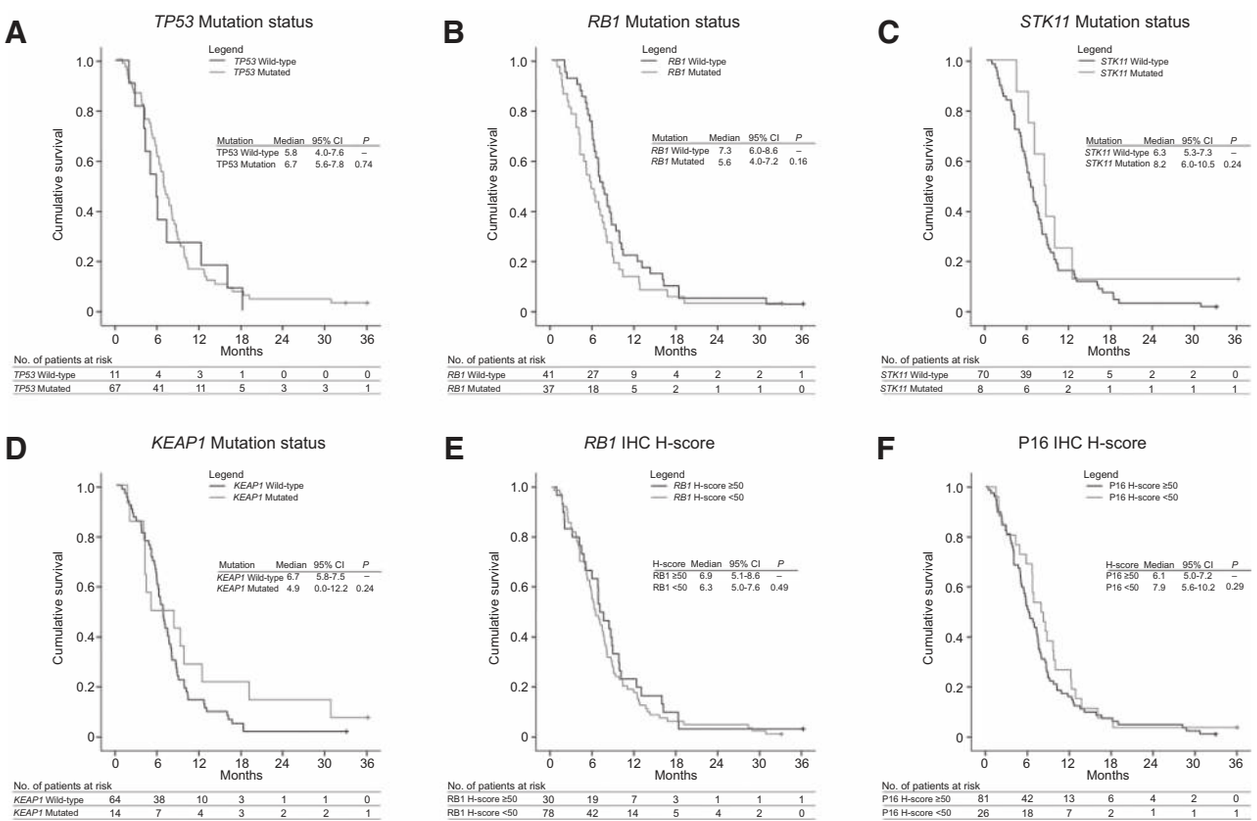

Figure 5.
A–D, Overall survival for mutational status in panel consensus LCNEC ($N = 78$)*. **E** and **F,** Overall survival in panel consensus LCNEC for RB1* ($N = 108$) and P16* ($N = 107$) IHC H-score. Abbreviations: No, number of. *, case 162 excluded for analyses.

in *RB1* and *STK11* occurred in a mutually exclusive way. The frequency of *STK11* mutations was lower than expected, probably due to the fact that with our approach we could only cover 60% of the coding region of this gene. Although the mutational status of the genes analyzed did not have a prognostic value, we observed that patients with *RB1* wild-type LCNECs showed a significant longer OS when treated with NSCLC-GEM/TAX compared with SCLC-PE and to NSCLC-PEM chemotherapies.

RB1 is inactivated in virtually all SCLCs but only in half of LCNECs (17, 33, 38–40). Similarly, RB1 protein expression is more frequently lost in SCLC (∼90%) than in LCNEC (45%–67%; refs. 17, 18, 35, 38, 41). However, its clinical relevance has not been assessed thoroughly but for a recent prospective study on SCLC reporting that patients with wild-type *RB1* but loss of the protein expression showed inferior OS and PFS when treated with SCLC-PE chemotherapy (42). In our study, we found that RB1 expression was completely lost in almost all *RB1*-mutated LCNECs, but also in 47% of the wild-type cases. Homozygous gene deletions measured by FISH did not explain the loss of expression in the wild-type samples. This suggests that protein expression might be a more reliable measurement of RB1 inactivation than mutation. In total, RB1 protein expression was strongly downregulated or completely lost in 72% of the LCNEC tumors analyzed, similarly to what has been reported in recent studies (17, 38). Similarly to *RB1* wild-type LCNEC patients, those with RB1-expressing tumors also showed a significant longer OS when treated with NSCLC-GEM/TAX than with SCLC-PE or NSCLC-PEM. But, in addition, Cox regression analysis confirmed the predictive value of RB1-positive staining on NSCLC-GEM/TAX versus SCLC-PE chemotherapy outcome, and PFS was also significantly longer for NSCLC-GEM/TAX versus SCLC-PE–treated patients.

P16 (*CDKN2A*) functions as an inhibitor of cyclin D-dependent kinases (CDK4/6) that phosphorylates RB1 enabling cell proliferation (43). *CDKN2A* (P16) and *RB1* inactivation seem to be mutually exclusive in LCNEC (18, 44), and their expression is strongly correlated; previous studies have indicated that combined low RB1 and high P16 proteins expression is observed in 45% to 78% of LCNEC and almost always in SCLC (>90%; refs. 35, 38, 41, 43). In our data, we have validated this patter, and we have additionally found that combined RB1 expression and loss of P16 expression are predictive for improved outcome on NSCLC-GEM/TAX chemotherapy treatment, although P16 staining did not show additive value to the RB1 staining alone.

Overall, we found that *RB1* mutational status and RB1/P16 protein expression are predictive markers for chemotherapy response and may aid to guide therapeutic decisions in advanced LCNEC disease. This is the largest (population-based) study evaluating chemotherapy outcome related to mutational patterns in panel-reviewed LCNECs. Although these results are of great interest for the clinical management of LCNEC, the few limitations of our study due to its retrospective design encourage the replication of these results in a prospective randomized clinical trial that stratifies LCNEC based on genomic subtypes and by RB1/P16 protein expression, and investigate outcome to NSCLC-GEM/TAX and SCLC-PE chemotherapy subtypes. In addition, these markers could be tested in biopsy specimens of high-grade neuroendocrine carcinomas to evaluate whether they could help in the differential diagnosis of LCNEC and SCLC.

Disclosure of Potential Conflicts of Interest

E.M. Speel reports receiving other commercial research support from Bristol-Myers Squibb. No potential conflicts of interest were disclosed by the other authors.

Authors' Contributions

Conception and design: J.L. Derks, E. Thunnissen, H.J.M. Groen, E.F. Smit, L. Fernandez-Cuesta, E.-J.M. Speel, A.-M.C. Dingemans

Development of methodology: J.L. Derks, E. Thunnissen, M. Foll, J.D. McKay, L. Fernandez-Cuesta, E.-J.M. Speel, A.-M.C. Dingemans

Acquisition of data (provided animals, acquired and managed patients, provided facilities, etc.): J.L. Derks, N. Leblay, E. Thunnissen, M. den Bakker, R. Damhuis, E.C. van den Broek, A. Chabrier, J.D. McKay, E.-J.M. Speel, A.-M.C. Dingemans

Analysis and interpretation of data (e.g., statistical analysis, biostatistics, computational analysis): J.L. Derks, N. Leblay, E. Thunnissen, R.J. van Suylen, H.J.M. Groen, R. Damhuis, M. Foll, L. Fernandez-Cuesta, E.-J.M. Speel, A.-M.C. Dingemans

Writing, review, and/or revision of the manuscript: J.L. Derks, E. Thunnissen, R.J. van Suylen, M. den Bakker, H.J.M. Groen, E.F. Smit, R. Damhuis, E.C. van den Broek, A. Chabrier, M. Foll, L. Fernandez-Cuesta, E.-J.M. Speel, A.-M.C. Dingemans

Administrative, technical, or material support (i.e., reporting or organizing data, constructing databases): J.L. Derks, E. Thunnissen, R.J. van Suylen, R. Damhuis, E.C. van den Broek, A. Chabrier, A.-M.C. Dingemans

Study supervision: L. Fernandez-Cuesta, E.-J.M. Speel, A.-M.C. Dingemans

Other (specimen review): M. den Bakker

Acknowledgments

We would like to thank G. Roemen and A. Haesevoets of the Department of Pathology of the Maastricht University Medical Centre (Maastricht, the Netherlands) for their help with performing the FISH analyses.

PALGA-group co-authors: L. Arensman, Meander Medisch Centrum Klinische Pathologie; F.E. Bellot, Klinische Pathologie Hoofddorp; J.E. Broers, Isala Klinieken; C.M. van Dish; Klinische pathologie Groene Hart Ziekenhuis; K.E.S.Duthoi, Amphia Ziekenhuis; M.J. Flens, Symbiant; J.M.M. Grefte, Gelre Ziekenhuis Klinische Pathologie; M.C.H. Hogenes, Labpon; R. Natté, Haga Ziekenhuis; A.F. van Hamel, Pathologie SSZOG; P.J.J.M. Klinkhamer, Stichting PAMM; J.W.R. Meijer, Ziekenhijs Rijnstate; J.C.C.van der Meij, Pathologie Friesland; F.H. van Nederveen Laboratorium voor Pathologie (PAL); E.W.P. Nijhuis, Onze Lieve Vrouwe Gasthuis; M.F.M. van Oosterhout, St. Antonius Ziekenhuis; S.H. Sastrowijoto, Pathologie Sittard; K. Schelfout, Stichting Pathologisch en Cytologisch Laboratorium West-Brabant; J. Sietsma, Pathologie Martini Ziekenhuis; F.M.M. Smedts, Reinier Haga MDC; M.M. Smits, Laboratorium voor Klinische Pathologie; J. Stavast, Laboratorium Klinische Pathologie Centraal Brabant; W. Timens, Pathologie UMCG; M.L. van Velthuysen, NKI-AVL; A. Vink, Universitair Medisch Centrum Utrecht; C.C.A.P. Wauters, Canisius Wilhelmina Ziekenhuis; S. Wouda, VieCuri Medical Centre.

Grant Support

This study was supported by grants from the Dutch Cancer Society (UM-2014-7110, to A-M. C. Dingemans). J.L. Derks is the recipient of an ERS/EMBO Joint Research Fellowship (STRTF 2016) 7178. The research leading to these results has received funding from the European Respiratory Society (ERS) and European Molecular Biology Organization (EMBO)".

The costs of publication of this article were defrayed in part by the payment of page charges. This article must therefore be hereby marked *advertisement* in accordance with 18 U.S.C. Section 1734 solely to indicate this fact.

Received July 10, 2017; revised September 12, 2017; accepted October 11, 2017; published OnlineFirst October 24, 2017.

References

1. Takei H, Asamura H, Maeshima A, Suzuki K, Kondo H, Niki T, et al. Large cell neuroendocrine carcinoma of the lung: a clinicopathologic study of eighty-seven cases. J Thorac Cardiovasc Surg 2002;124:285–92.
2. Derks JL, Hendriks LE, Buikhuisen WA, Groen HJ, Thunnissen E, van Suylen RJ, et al. Clinical features of large cell neuroendocrine carcinoma: a population-based overview. Eur Respir J 2016;47:615–24.
3. Asamura H, Kameya T, Matsuno Y, Noguchi M, Tada H, Ishikawa Y, et al. Neuroendocrine neoplasms of the lung: a prognostic spectrum. J Clin Oncol 2006;24:70–6.
4. Travis WD, Brambilla E, Burke AP, Marx A, Nicholson AG. WHO Classification of Tumours of the Lung, Pleura, Thymus and Heart. Fourth edition. In: WHO Classification of Tumours. Geneva, Switzerland: World Health Organization; 2015.
5. Travis WD, Linnoila RI, Tsokos MG, Hitchcock CL, Cutler GB Jr, Nieman L, et al. Neuroendocrine tumors of the lung with proposed criteria for large-cell neuroendocrine carcinoma. An ultrastructural, immunohistochemical, and flow cytometric study of 35 cases. Am J Surg Pathol 1991;15:529–53.
6. Travis WD, Gal AA, Colby TV, Klimstra DS, Falk R, Koss MN. Reproducibility of neuroendocrine lung tumor classification. Hum Pathol 1998; 29:272–9.
7. Den Bakker MA, Willemsen S, Grunberg K, Noorduijn LA, Van Oosterhout MFM, Van Suylen RJ, et al. Small cell carcinoma of the lung and large cell neuroendocrine carcinoma interobserver variability. Histopathology 2010;56:356–63.
8. Thunnissen E, Borczuk AC, Flieder DB, Witte B, Beasley MB, Chung JH, et al. The use of immunohistochemistry improves the diagnosis of small cell lung cancer and its differential diagnosis. An international reproducibility study in a demanding set of cases. J Thorac Oncol 2017;12:334–46.
9. Marchevsky AM, Gal AA, Shah S, Koss MN. Morphometry confirms the presence of considerable nuclear size overlap between "small cells" and "large cells" in high-grade pulmonary neuroendocrine neoplasms. Am J Clin Pathol 2001;116:466–72.
10. Fabbri A, Cossa M, Sonzogni A, Papotti M, Righi L, Gatti G, et al. Ki-67 labeling index of neuroendocrine tumors of the lung has a high level of correspondence between biopsy samples and surgical specimens when strict counting guidelines are applied. Virchows Arch 2017;470:153–64.
11. Nicholson SA, Beasley MB, Brambilla E, Hasleton PS, Colby TV, Sheppard MN, et al. Small cell lung carcinoma (SCLC): a clinicopathologic study of 100 cases with surgical specimens. Am J Surg Pathol 2002; 26:1184–97.
12. Derks JL, Jan van Suylen R, Thunnissen E, den Bakker MA, Smit EF, Groen HJ, et al. A population-based analysis of application of WHO nomenclature in pathology reports of pulmonary neuroendocrine tumors. J Thorac Oncol 2016;11:593–602.
13. Masters GA, Temin S, Azzoli CG, Giaccone G, Baker S Jr, Brahmer JR, et al. Systemic therapy for stage IV non-small-cell lung cancer: American Society of Clinical Oncology Clinical Practice Guideline Update. J Clin Oncol 2015;33:3488–515.
14. Derks JL, van Suylen RJ, Thunnissen E, den Bakker MA, Groen HJ, Smit EF, et al. Chemotherapy for pulmonary large cell neuroendocrine carcinomas: does the regimen matter? Eur Respir J 2017;49:160183.
15. Naidoo J, Santos-Zabala ML, Lyriboz T, Woo KM, Sima CS, Fiore JJ, et al. Large cell neuroendocrine carcinoma of the lung: clinicopathologic features, treatment, and outcomes. Clin Lung Cancer 2016; 17:e121–9.
16. Christopoulos P, Engel-Riedel W, Grohe C, Kropf-Sanchen C, von Pawel J, Gutz S, et al. Everolimus with paclitaxel and carboplatin as first-line treatment for metastatic large-cell neuroendocrine lung carcinoma: a multicenter phase II trial. Ann Oncol 2017;28:1898–902.
17. Rekhtman N, Pietanza MC, Hellmann M, Naidoo J, Arora A, Won H, et al. Next-generation sequencing of pulmonary large cell neuroendocrine carcinoma reveals small cell carcinoma-like and non-small cell carcinoma-like subsets. Clin Cancer Res 2016;22:3618–29.
18. George J, Fernandez-Cuesta L, Vonn W, Hayes N, Thomas RK. Comparative analysis of small cell lung cancer and other pulmonary neuroendocrine tumors. Cancer Res 2016;76(14 suppl):122.
19. Casparie M, Tiebosch AT, Burger G, Blauwgeers H, van de Pol A, van Krieken JH, et al. Pathology databanking and biobanking in The Netherlands, a central role for PALGA, the nationwide histopathology and cytopathology data network and archive. Cell Oncol 2007;29: 19–24.
20. Socinski MA, Smit EF, Lorigan P, Konduri K, Reck M, Szczesna A, et al. Phase III study of pemetrexed plus carboplatin compared with etoposide plus carboplatin in chemotherapy-naive patients with extensive-stage small-cell lung cancer. J Clin Oncol 2009;27:4787–92.
21. Hou J, Lambers M, den Hamer B, den Bakker MA, Hoogsteden HC, Grosveld F, et al. Expression profiling-based subtyping identifies novel non-small cell lung cancer subgroups and implicates putative resistance to pemetrexed therapy. J Thorac Oncol 2012;7: 105–14.
22. Monica V, Scagliotti GV, Ceppi P, Righi L, Cambieri A, Lo Iacono M, et al. Differential thymidylate synthase expression in different variants of large-cell carcinoma of the lung. Clin Cancer Res 2009; 15:7547–52.
23. Ceppi P, Volante M, Ferrero A, Righi L, Rapa I, Rosas R, et al. Thymidylate synthase expression in gastroenteropancreatic and pulmonary neuroendocrine tumors. Clin Cancer Res 2008;14:1059–64.
24. Rindi G, Klersy C, Inzani F, Fellegara G, Ampollini L, Ardizzoni A, et al. Grading the neuroendocrine tumors of the lung: an evidence-based proposal. Endocr Relat Cancer 2014;21:1–16.
25. Li H, Handsaker B, Wysoker A, Fennell T, Ruan J, Homer N, et al. The Sequence Alignment/Map format and SAMtools. Bioinformatics 2009;25: 2078–9.
26. Fernandez-Cuesta L, Perdomo S, Avogbe PH, Leblay N, Delhomme TM, Gaborieau V, et al. Identification of circulating tumor DNA for the early detection of small-cell lung cancer. EBioMedicine 2016; 10:117–23.
27. Wang K, Li M, Hakonarson H. ANNOVAR: functional annotation of genetic variants from high-throughput sequencing data. Nucleic Acids Res 2010;38:e164.
28. Sim NL, Kumar P, Hu J, Henikoff S, Schneider G, Ng PC. SIFT web server: predicting effects of amino acid substitutions on proteins. Nucleic Acids Res 2012;40:W452–7.
29. Adzhubei IA, Schmidt S, Peshkin L, Ramensky VE, Gerasimova A, Bork P, et al. A method and server for predicting damaging missense mutations. Nat Methods 2010;7:248–9.
30. Lek M, Karczewski KJ, Minikel EV, Samocha KE, Banks E, Fennell T, et al. Analysis of protein-coding genetic variation in 60,706 humans. Nature 2016;536:285–91.
31. Exome Variant Server. NHLBI GO Exome Sequencing Project (ESP); 2017. Available from: http://evs.gs.washington.edu/EVS/.
32. Abecasis GR, Altshuler D, Auton A, Brooks LD, Durbin RM, Gibbs RA, et al. A map of human genome variation from population-scale sequencing. Nature 2010;467:1061–73.
33. George J, Lim JS, Jang SJ, Cun Y, Ozretic L, Kong G, et al. Comprehensive genomic profiles of small cell lung cancer. Nature 2015;524: 47–53.
34. Shapiro GI, Edwards CD, Kobzik L, Godleski J, Richards W, Sugarbaker DJ, et al. Reciprocal Rb inactivation and p16INK4 expression in primary lung cancers and cell lines. Cancer Res 1995;55:505–9.
35. Beasley MB, Lantuejoul S, Abbondanzo S, Chu WS, Hasleton PS, Travis WD, et al. The P16/cyclin D1/Rb pathway in neuroendocrine tumors of the lung. Hum Pathol 2003;34:136–42.
36. Le Treut J, Sault MC, Lena H, Souquet PJ, Vergnenegre A, Le Caer H, et al. Multicentre phase II study of cisplatin-etoposide chemotherapy for advanced large-cell neuroendocrine lung carcinoma: the GFPC 0302 study. Ann Oncol 2013;24:1548–52.
37. Niho S, Kenmotsu H, Sekine I, Ishii G, Ishikawa Y, Noguchi M, et al. Combination chemotherapy with irinotecan and cisplatin for large-cell neuroendocrine carcinoma of the lung: a multicenter phase II study. J Thorac Oncol 2013;8:980–4.
38. Miyoshi T, Umemura S, Matsumura Y, Mimaki S, Tada S, Ishii G, et al. Genomic profiling of large-cell neuroendocrine carcinoma of the lung. Clin Cancer Res 2016;23:757–65.
39. Karlsson A, Brunnstrom H, Lindquist KE, Jirstrom K, Jonsson M, Rosengren F, et al. Mutational and gene fusion analyses of primary

large cell and large cell neuroendocrine lung cancer. Oncotarget 2015;6:22028–37.
40. Simbolo M, Mafficini A, Sikora KO, Fassan M, Barbi S, Corbo V, et al. Lung neuroendocrine tumours: deep sequencing of the four World Health Organization histotypes reveals chromatin-remodelling genes as major players and a prognostic role for TERT, RB1, MEN1 and KMT2D. J Pathol 2017;241:488–500.
41. Igarashi T, Jiang SX, Kameya T, Asamura H, Sato Y, Nagai K, et al. Divergent cyclin B1 expression and Rb/p16/cyclin D1 pathway aberrations among pulmonary neuroendocrine tumors. Mod Pathol 2004; 17:1259–67.
42. Dowlati A, Lipka MB, McColl K, Dabir S, Behtaj M, Kresak A, et al. Clinical correlation of extensive-stage small-cell lung cancer genomics. Ann Oncol 2016;27:642–7.
43. Otterson GA, Kratzke RA, Coxon A, Kim YW, Kaye FJ. Absence of p16INK4 protein is restricted to the subset of lung cancer lines that retains wildtype RB. Oncogene 1994;9:3375–8.
44. Kwang Chae Y, Tamragouri K, Chung J, Schrock AB, Kolla B, Ganesan S, et al. Genomic alterations (GA) and tumor mutational burden (TMB) in large cell neuroendocrine carcinoma of lung (L-LCNEC) as compared to small cell lung carcinoma (SCLC) as assessed via comprehensive genomic profiling (CGP). J Clin Oncol 35:15s, 2017(suppl; abstr 8517).